

## INVESTIGATION ON THE VIBRATIONAL SPECTRA AND GEOMETRY OF FLUAZINAM: A DFT MODUS

**R. GODWINI, J.**, Reg.No:19123092132022, Research Scholar, Department of Physics and Research Centre, Women's Christian College, Nagercoil-629001, Tamil Nadu, India.

**CLEMY MONICKA**, Assistant Professor, Department of Physics, St. John's College of Arts and Science, Ammandivilai-629204, Tamil Nadu, India. Affiliated to Manonmaniam Sundaranar University, Abishekapatti-627012, Tirunelveli, Tamil Nadu, India., monika@stjohns.ac.in

**S. GRACE VICTORIA**, Assistant Professor, Department of Physics and Research Centre, Women's Christian College, Nagercoil-629001, Tamil Nadu, India.

**ABSTRACT-** The designated compound has been inspected through quantum chemical computations and the geometry of which is optimized to minimum energy configuration by B3LYP/6-311 ++ G (d, p) basis set employing DFT approach. Electron transfer from donor to acceptor orbitals has been analysed through Natural bond Orbital (NBO) analysis. Vibrational modes were assigned based on Potential Energy Distribution (PED) contribution. In the optimized geometry, C-N bond length displays a double bond nature due to the transfer of lone pair electron from amide group nitrogen to the pyridine ring which is also justified in the natural bond analysis.

**Key Words-** DFT, Topology Analysis.

### 1. INTRODUCTION

The headline compound Fluazinam, adopted for the present inspection belongs to the class of pyridine amine fungicides [1]. Pyridine and its derivatives scored diverse applications in pharmaceuticals. Assessment of the literature has revealed that there's been no substantial theoretical quantum chemical research incorporated with the vibrational spectra of the specified molecule reported to date. Hence quantum chemical investigation on the structure of Fluazinam has been initiated using the DFT approach.

### 2. SPECTRAL PROFILE

Sigma Aldrich Scientific Company offered the sample of Fluazinam in powder form which is used without further purification. Bruker: RFS 27 standalone FT-Raman spectrometer is used to record the FT-Raman spectra of the sample in the zone 4000-100  $\text{cm}^{-1}$ . The sample was subjected to a Laser excitation source of 200 mW and the spectrum was obtained with 1  $\text{cm}^{-1}$  resolution. FT-Infrared spectrum in the range 4000-500  $\text{cm}^{-1}$  was captured using Perkin Elmer spectrometer with 1  $\text{cm}^{-1}$  spectral resolution.

### 3. SIMULATION METHODOLOGIES

The Density functional theoretical approach embedded with B3LYP functional and the basis set 6-311 G (d, p) with ++ diffuse function has served as a foundation for all computations in the present investigation. Geometry of Fluazinam has been subjected to optimization using Gaussian 09 software [12]. Vibrational bands were assigned based on the Potential Energy distribution (PED) using MOLVIB Program version 7.0 [14]. Donor- acceptor interactions were carried out using NBO version 3.1 [15].

### 4. RESULTS AND DISCUSSION

#### 4.1. Geometry Optimization

The molecular structure of Fluazinam comprises a poly-substituted phenyl ring a di substituted pyridine ring linked by an amide group. Optimized geometry of Fluazinam is shown in Fig 1. In the optimized geometrical structure, electronegative chlorine atoms in adjunction with the phenyl and pyridine rings at positions C<sub>5</sub> and C<sub>26</sub> brings about an upsurge in the C-C bond lengths C<sub>5</sub>-C<sub>6</sub> (1.4017 Å) and C<sub>21</sub>-C<sub>26</sub> (1.4115Å) [19]. The corresponding deviations from the normal C=C bond length of 1.39 Å are 0.0117 Å and 0.0215Å respectively. N<sub>19</sub>-H<sub>20</sub> bond length is lengthened from the experimental value due to weak intra-molecular hydrogen bonding N<sub>19</sub>-H<sub>20</sub>-O<sub>14</sub>.

TABLE I: Optimized Bond Lengths, Bond Angles and Dihedral Angles of Fluazinam Calculated at B3LYP/6-311++ G (D, P) Level

Bond Length	Experimental Å	Theoretical Å	Bond Angle & Dihedral angle	Experimental (°)	Theoretical (°)
C <sub>1</sub> -C <sub>6</sub>	1.38	1.38	C <sub>2</sub> -C <sub>1</sub> -C <sub>6</sub>	120.52	121.49
C <sub>2</sub> -C <sub>3</sub>	1.39	1.40	C <sub>2</sub> -C <sub>3</sub> -C <sub>4</sub>	115.13	115.31
C <sub>3</sub> -N <sub>19</sub>	1.39	1.38	C <sub>4</sub> -C <sub>5</sub> -Cl <sub>11</sub>	119.38	120.02
O <sub>12</sub> -N <sub>13</sub>	1.20	1.21	C <sub>6</sub> -C <sub>7</sub> -F <sub>9</sub>	111.11	112.04
N <sub>13</sub> -O <sub>14</sub>	1.19	1.22	C <sub>6</sub> -C <sub>1</sub> -C <sub>2</sub> -C <sub>3</sub>	3.49	3.50
N <sub>19</sub> -H <sub>20</sub>	0.88	1.01	C <sub>2</sub> -C <sub>1</sub> -C <sub>6</sub> -C <sub>5</sub>	-0.86	-2.00

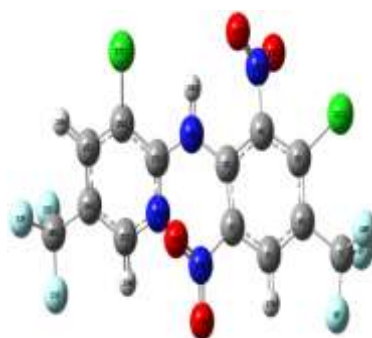


Fig 1 Optimized structure of Fluazinam with atom numbering scheme

#### 4.2. NBO Analysis

Natural bond orbital analysis claims to be an effectual tackle in ascertaining intra molecular charge transfer between the filled and unfilled orbitals, hydrogen bonding in terms of stabilisation energies. The strength of interactions proportional to the stabilisation energies are indexed in Table II by means of second order fock matrix.  $E(2)$  means energy of hyper conjugative interactions.  $E(j)-E(i)$  is the Energy difference between donor and acceptor  $i$  and  $j$  NBO orbitals.  $F(i, j)$  is the Fock matrix element between  $i$  and  $j$  NBO orbitals. Lone pair electrons from LP (1) N<sub>19</sub> interacting with the anti-bonding orbital  $\pi^*$  (C<sub>21</sub>-N<sub>22</sub>) accord utmost stabilisation energy of 187.1 kJ/mol and hence the occupancy of the bonded orbital increases to an extent of 0.4465e. Abatement in the C<sub>21</sub>-N<sub>22</sub> (0.16 Å) bond length further confirms this interaction.

TABLE II

Second Order Perturbation Theory Analysis of Fock Matrix in NBO Basis

Donor	ED (i) e	Acceptor	ED (j) e	E(2) kJ/mol	E(j)-E(i) a.u	F(i, j) a.u
$\pi$ (C <sub>1</sub> -C <sub>6</sub> )	1.65586	$\pi^*$ (C <sub>2</sub> -C <sub>3</sub> )	0.4289 1	70.37	0.27	0.062
$\pi$ (C <sub>1</sub> -C <sub>6</sub> )	1.65586	$\pi^*$ (C <sub>4</sub> -C <sub>5</sub> )	0.4281 8	106.6 0	0.26	0.074
$\pi$ (C <sub>21</sub> -N <sub>22</sub> )	1.71647	$\pi^*$ (C <sub>23</sub> -C <sub>24</sub> )	0.3262 3	115.0 5	0.34	0.087
LP (1) N <sub>19</sub>	1.68708	$\pi^*$ (C <sub>21</sub> -N <sub>22</sub> )	0.4465 1	44.73	0.27	0.102
LP (3) O <sub>14</sub>	1.43474	$\sigma^*$ (N <sub>19</sub> -H <sub>20</sub> )	0.0293 4	7.86	0.68	0.037

### 4.3. Vibrational Assignments

#### 4.3.1 Phenyl Ring Vibrations

Poly substituted phenyl rings show modes 8a, 8b, 19a, 19b and 14 in accordance to Wilson's numbering scheme for C-C stretching vibrations [27]. The frequency limit for vibrational mode 8 is 1520- 1650  $\text{cm}^{-1}$ . Mode 8a is noted at 1504  $\text{cm}^{-1}$  whereas mode 8b is observed at 1614  $\text{cm}^{-1}$  in the Raman Spectra. Mode 19a – 19b generally occurs in between 1364-1428  $\text{cm}^{-1}$ .

#### 4.3.2 Pyridine Ring Vibrations

Peak observed at 3072  $\text{cm}^{-1}$  in the Raman spectra is assigned to C-H stretching vibration with PED contribution assigned is 99%. Interaction between C-C and C-N stretching vibrations result in strong to medium absorption bands between 1615-1575  $\text{cm}^{-1}$  and 1520-1465  $\text{cm}^{-1}$ .

#### 4.3.3 N-H Vibrations

Hetero aromatic compounds gives rise to bands between 3500 and 3300  $\text{cm}^{-1}$ . The band noticed at 3387  $\text{cm}^{-1}$  in the IR spectra is assigned to fundamental N-H stretching vibration which is 100% contributed based on PED.

#### 4.3.4 Nitro Group Vibrations

Aromatic compounds with nitro group substitution absorb strongly at 1570-1485  $\text{cm}^{-1}$  and 1370-1320  $\text{cm}^{-1}$ . Asymmetric stretching vibration is observed at 1574  $\text{cm}^{-1}$  and 1539  $\text{cm}^{-1}$  (IR) and 1544  $\text{cm}^{-1}$  (Raman). **4.3.5 Methyl Group Vibrations-** C-F stretching vibrations are observed in 1123  $\text{cm}^{-1}$  in the IR spectra and the Raman spectra shows its analogue at 1126  $\text{cm}^{-1}$  with 49% PED contribution.

## 5. CONCLUSION

A detailed exploration of the structure of Fluazinam was accomplished with the aid of Quantum chemical computation methodology as well as vibrational spectroscopic techniques. The nature and strength of the bonds formed by hydrogen bonding are explained by optimized geometry, as is the deviation of optimized parameters from standard values. The importance of electronegative substituents governing geometry is also warranted by NBO analysis.

### ACKNOWLEDGEMENT

The Authors express their gratitude towards the Department of Physics, University of Kerala, for providing with the Gaussian Software for computational work

### REFERENCES

- [1] Y. Jeon, J. Kim, S. Lee, and T. H. Kim. (2013).Fluazinam. Acta Crystallogr. Sect. E Struct. Reports Online, 69 (9), 171–177.
- [2] M. J. Frisch, G. W. Trucks, H. B. Schlegel et al., "Gaussian 09." Gaussian, Inc., Wallingford CT, 2009.
- [3] T. Sundius.(2002).Scaling of ab initio force fields by MOLVIB. Vib. Spectrosc., 29(1–2),89–95.
- [4] E. D. Glendening, C. R. Landis, and F. Weinhold.(2012).Natural bond orbital methods.Wiley Interdiscip. Rev. Comput. Mol. Sci,2 (1),1–42.
- [5] S. J. J. Mary, M. U. M. Siddique, S. Pradhan, V. Jayaprakash, and C. James.(2021).Quantum chemical insight into molecular structure, NBO analysis of the hydrogen-bonded interactions, spectroscopic (FT–IR, FT–Raman), drug likeness and molecular docking of the novel anti COVID-19 molecule 2-[(4,6-diaminopyrimidin-2-imer," *Spectrochim. Acta - Part A Mol. Biomol. Spectrosc.*, 244, 118825.